International Journal of River Basin Management
Publication details, including instructions for authors and subscription information:
http://www.tandfonline.com/loi/trbm20

Development of statistically unbiased twenty-first century hydrology scenarios over La Plata Basin

Ramiro I. Saurral[ab], Natalia B. Montroull[ac] & Inés A. Camilloni[ac]

[a] Departamento de Ciencias de la Atmósfera y los Océanos (DCAO, FCEN-UBA), Buenos Aires, Argentina

[b] Centro de Investigaciones del Mar y la Atmósfera (CIMA, UBA-CONICET), UMI-IFAECI/CNRS, Int. Güiraldes 2160, Ciudad Universitaria, Pab. 2 (C1428EGA), Buenos Aires, Argentina.

[c] Centro de Investigaciones del Mar y la Atmósfera (CIMA, UBA-CONICET), UMI-IFAECI/CNRS, Int. Güiraldes 2160, Ciudad Universitaria, Pab. 2 (C1428EGA), Buenos Aires, Argentina.

Accepted author version posted online: 05 Feb 2014.Published online: 28 Feb 2013.

To cite this article: Ramiro I. Saurral, Natalia B. Montroull & Inés A. Camilloni (2013) Development of statistically unbiased twenty-first century hydrology scenarios over La Plata Basin, International Journal of River Basin Management, 11:4, 329-343, DOI: 10.1080/15715124.2014.885440

To link to this article: http://dx.doi.org/10.1080/15715124.2014.885440

Intl. J. River Basin Management Vol. 11, No. 4 (December 2013), pp. 329–343

Research paper

Development of statistically unbiased twenty-first century hydrology scenarios over La Plata Basin

RAMIRO I. SAURRAL, *Departamento de Ciencias de la Atmósfera y los Océanos (DCAO, FCEN-UBA), Buenos Aires, Argentina; Centro de Investigaciones del Mar y la Atmósfera (CIMA, UBA-CONICET), UMI-IFAECI/CNRS, Int. Güiraldes 2160, Ciudad Universitaria, Pab. 2 (C1428EGA), Buenos Aires, Argentina. Email: saurral@cima.fcen.uba.ar (author for correspondence)*

NATALIA B. MONTROULL, *Departamento de Ciencias de la Atmósfera y los Océanos (DCAO, FCEN-UBA), Buenos Aires, Argentina; Centro de Investigaciones del Mar y la Atmósfera (CIMA, UBA-CONICET), UMI-IFAECI/CNRS, Int. Güiraldes 2160, Ciudad Universitaria, Pab. 2 (C1428EGA), Buenos Aires, Argentina.*

INÉS A. CAMILLONI, *Departamento de Ciencias de la Atmósfera y los Océanos (DCAO, FCEN-UBA), Buenos Aires, Argentina; Centro de Investigaciones del Mar y la Atmósfera (CIMA, UBA-CONICET), UMI-IFAECI/CNRS, Int. Güiraldes 2160, Ciudad Universitaria, Pab. 2 (C1428EGA), Buenos Aires, Argentina.*

ABSTRACT

There is an increasing demand for future climate scenarios, particularly for impact studies. In this study, simulation outputs taken from a set of three regional climate models (RCMs) are used to force a hydrologic model to derive future streamflow scenarios for La Plata Basin. As RCMs have biases in their mean precipitation and temperature fields, a statistical scheme is previously used to remove the systematic part of the bias. Future hydrologic scenarios were derived considering two future periods: 2021–2040 (near future) and 2071–2090 (far future). In terms of climate projections, RCMs predict warmer conditions in almost the whole basin, while precipitation variations are not uniform in sign across the region but overall tend to be positive over the southern part of the basin. Nevertheless, a trend towards a gradual increase in streamflow was found for the majority of the rivers in the basin particularly for the near future followed by less uniform variations towards the end of the present century. Future changes in the largest monthly streamflow are similar to those in the mean values, with also some differences among RCMs and on the period and sub-basin considered.

Keywords: La Plata Basin; regional climate models; future hydrology scenarios; impact studies

1 Introduction

Fresh water availability is one of the largest challenges in the face of climate change for the present century (Solomon *et al*. 2007). Variations in climate conditions, mainly in precipitation, temperature, evaporation and runoff, as well as changes in land cover could lead to noticeable modifications in the hydrologic cycle. These changes would naturally have a deeper effect over the largest freshwater basins among which La Plata Basin (LPB) is found.

LPB, located in South America, is the fifth largest fresh water basin in the world. With an area of more than 3 million km^2, it covers parts of five countries: Argentina, Brazil, Bolivia, Paraguay and Uruguay. With over 100 million inhabitants, 50 big cities, 75 dams and more than 30 large hydropower plants, LPB is at the core of the region's socio-economic activities, which generate around 70% of the *per capita* Gross Domestic Product of the five countries. Current basin hydropower production is 309,503 GWh, which contributes 55.5% of the total energy demand in LPB (Popescu *et al*. 2012). The basin is sensitive to well-known modes of climate variability in the Southern Hemisphere as El Niño-Southern Oscillation (ENSO; Ropelewski and Halpert 1987, Grimm *et al*. 2000) and the Southern Annual Mode (Silvestri and Vera 2003) and it has experienced significant positive precipitation trends in the last few decades (Castañeda and Barros 1994, Barros *et al*. 2008) which led to large increases in river discharges (Bischoff *et al*. 2000, Barros *et al*. 2004, Doyle and Barros 2011). Recent

Received 27 February 2013. Accepted 16 January 2014.

ISSN 1571-5124 print/ISSN 1814-2060 online
http://dx.doi.org/10.1080/15715124.2014.885440
http://www.tandfonline.com

studies have shown that these trends in rainfall are mainly explained by a significant increase in heavy precipitation events (above the 95th percentile; Doyle *et al*. 2012). An arising question here is whether these positive trends will persist into the future, leading to an intensification of the hydrologic cycle, or if they will reverse.

The objective of this paper is to assess the possible variations in the hydrologic cycle of LPB making focus on precipitation, temperature and river discharges for the next decades. A set of regional climate models (RCMs) forced with greenhouse gases and aerosols concentrations following the A1B emission scenario defined in the IPCC's Special Report on Emission Scenarios (see Solomon *et al*. 2007 for further details) provide daily precipitation and temperature fields for the period 1991–2090. These meteorological fields are used to force a semi-distributed hydrologic model which derives surface and sub-surface runoff and associated discharges at points in selected rivers. Variations in river discharges for the upcoming decades are quantified.

This paper is organized as follows: Section 2 describes the RCM data set as well as the hydrologic model used in this study along with the methodologies. Results and discussion are included in Section 3, while conclusions are described in Section 4.

2 Data and methodology

2.1 *Regional climate models*

This paper considers a set of three RCM simulations that were derived by Working Package 5 during the development of the European-South American CLARIS Research Project on Climate Change Impact over the LPB region (http://www.claris-eu.org). These RCMs are nested in different global climate models (GCMs) from which they get the boundary conditions (BC) and which consider the same emission scenario – A1B – to simulate future climate. Table 1 lists information on the RCMs as well as the time periods used as 'present climate' and 'future climate'. The need for high temporal resolution and, at the same time, the limitations due to computational resources during the CLARIS Project resulted as a compromise in the selection of three distinct periods, representatives of the 'present climate', the 'near future' and 'far future' conditions, respectively: 1991–2000, 2021–2040 and 2071–2090. Although a 10-year period can be considered too short to be representative of the actual conditions, the selection of this length resulted once again from the compromise in the project between ideal and doable simulations.

Daily information on minimum and maximum temperature, precipitation, wind speed, relative humidity and long- and short-wave incoming radiation were available from the RCMs and used to force the hydrologic model (see Section 2.2). It is worth mentioning that although the Swedish Meteorological and Hydrological Institute (SMHI) and the Universidad de Castilla-La Mancha (UCLM) made available climate simulations from their RCMs (RCA and PROMES, respectively) with no interruptions from 1991 to 2100, periods 2021–2040 and 2071–2090 were common to the three RCMs and were chosen for better comparison.

RCM outputs in the present climate were validated against observations using the Climate Research Unit (CRU) v3.1 data set developed following the methodology of Mitchell and Jones (2005) as a proxy of the observed climate. The period chosen to derive a 'present climate' was 1991–2000 and the meteorological variables considered were monthly mean temperature and accumulated precipitation covering the LPB region.

Figure 1 shows annual, austral summer (December–January–February; DJF) and austral winter (June–July–August; JJA) mean and standard deviation of monthly precipitation in the four RCMs and in the CRU data set (hereinafter referred to as 'observations'). In the annual scale (top row), the RCMs represent adequately the east-west precipitation gradient, with rainfall maxima to the east of the LPB region with values of about 150–200 mm month^{-1} (near 2000 mm year^{-1}). In the observations, two distinct maxima are found east of 60°W, one centred near 20°S related to the South Atlantic Convergence Zone (SACZ; Kodama 1992) and the other one between 25°S and 30°S linked to synoptic-scale activity (Vera *et al*. 2002). These maxima are explained by excessive rainfall during the warm and cold seasons, respectively (see middle and bottom

Table 1 List of RCMs and respective BC obtained from GCMs for present and future periods

RCMs	Institution (country)	BC (GCMs)	Time slices		References
			Present	Future	
PROMES (PROgnostic at the MESoscale)	Universidad de Castilla-La Mancha (Spain)	HadCM3	1991–2000	2021–2040 2071–2090	Sánchez *et al*. (2007) and Domínguez *et al*. (2010)
RCA (Rossby Centre RCM)	Swedish Meteorological and Hydrological Institute (Sweden)	ECHAM5			Kjellström *et al*. (2005) and Samuelsson *et al*. (2006)
LMDZ Modèle de Circulation Générale du LMD	Laboratoire de Meteorologie Dynamique (France)	LMDZ global			Li (1999) and Hourdin *et al*. (2006)

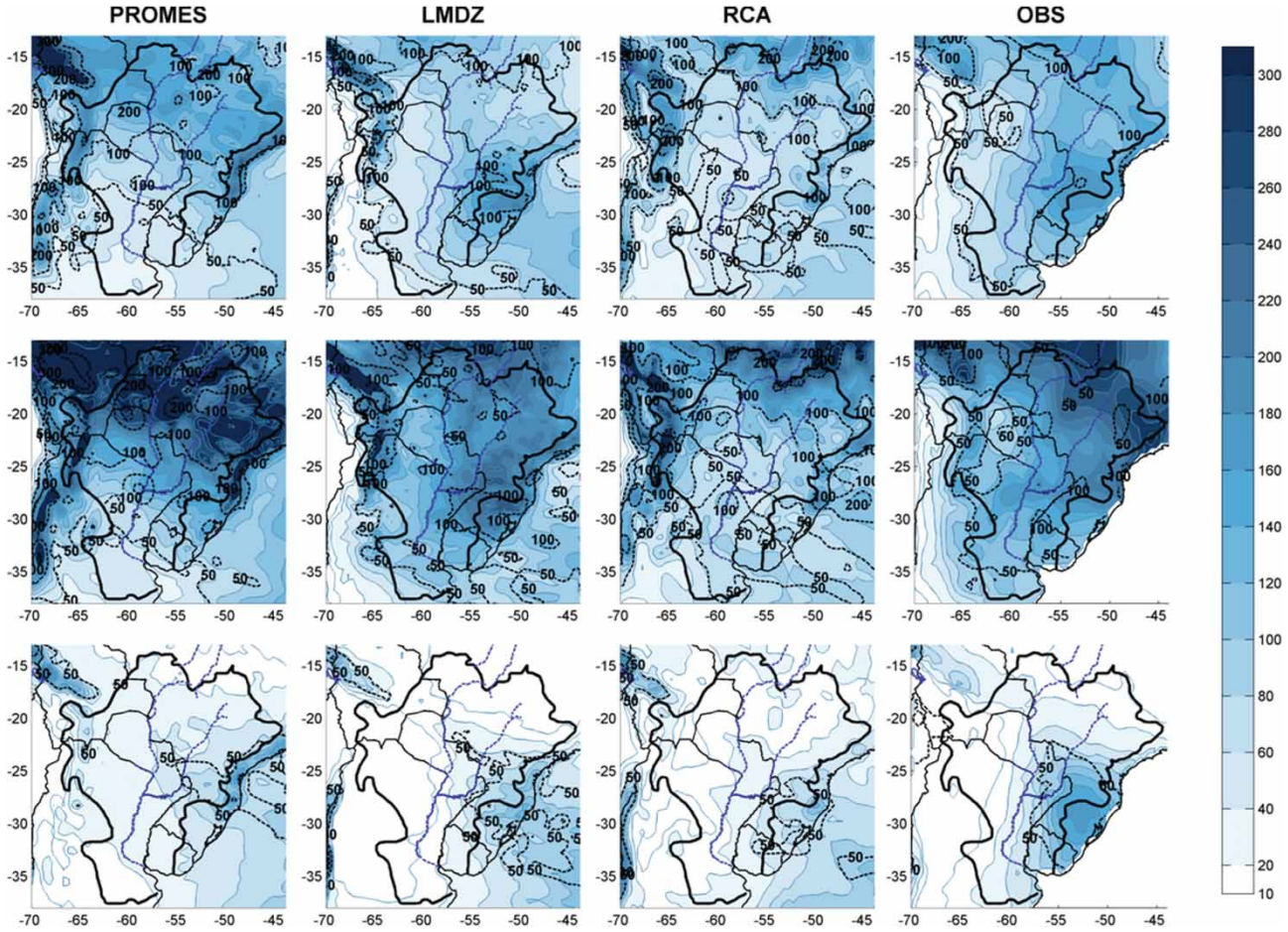

Figure 1 Annual (top), DJF (middle) and JJA (bottom) mean (shaded) and standard deviation (dashed black lines) of precipitation in PROMES, LMDZ and RCA (first to third columns, respectively), and in the observations (fourth column). Units are mm month^{-1}. Dashed blue lines depict the main rivers of the region (see Figure 3 for more details).

rows in the observations column). RCMs can simulate enhanced rainfall in the eastern half of the LPB domain although the location and magnitude of the rainfall maximum differ among the models. For instance, LMDZ depicts a single rainfall maximum near 30°S while PROMES concentrates more rainfall in the SACZ region. This is not surprising since the last two models use Hadley Centre version 3 GCM as BC and this GCM underestimates rainfall in the south of the basin (Vera *et al*. 2006, Gulizia *et al*. 2012). As is the case with GCMs (Saurral 2010), the most prominent error in the simulations of rainfall in the RCMs considered in this paper is the notorious dry patter in the cold season (JJA) in the south of the basin. RCMs do simulate a maximum of precipitation there but located east of the actual site. Among the four RCMs, LMDZ is the one who places this maximum closest to the observations. Standard deviation of precipitation is well represented in general by all RCMs. However, PROMES in summer (DJF) simulates excessive variability over subtropical South America, centred between 15°S and 25°S, compared to the observations. An important point to mention here is that RCMs simulate large rainfall values over the Andes particularly in summer which are inconsistent with the observations and could be explained by the poor spatial coverage of precipitation gauges over the Andes.

In terms of temperature differences (Figure 2), PROMES and RCA are warmer than the observations, with differences of about 2–3°C in the central part of the basin in both the annual and summer fields. On the other hand, LMDZ is closer to the observations in the annual field and somewhat cooler in both summer and winter. Standard deviation fields in the RCMs are similar to the observations, although once again PROMES overestimates its magnitude in general and especially in summer. These errors in both precipitation and temperature pose restrictions to the use of the RCMs for hydrologic assessments, and highlight the necessity of application of correction schemes to remove the systematic biases in the meteorological fields prior to their use in impact studies. This issue will be addressed in detail in Section 2.3.

2.2 *Hydrology model*

The variable infiltration capacity (VIC) hydrologic model (Liang *et al*. 1994, 1996, Nijssen *et al*. 1997), developed at the Department of Civil Engineering of the University of Washington, USA, is a distributed land surface scheme that solves both water and energy balances on a grid mesh. It simulates the main components of the surface and sub-surface hydrologic

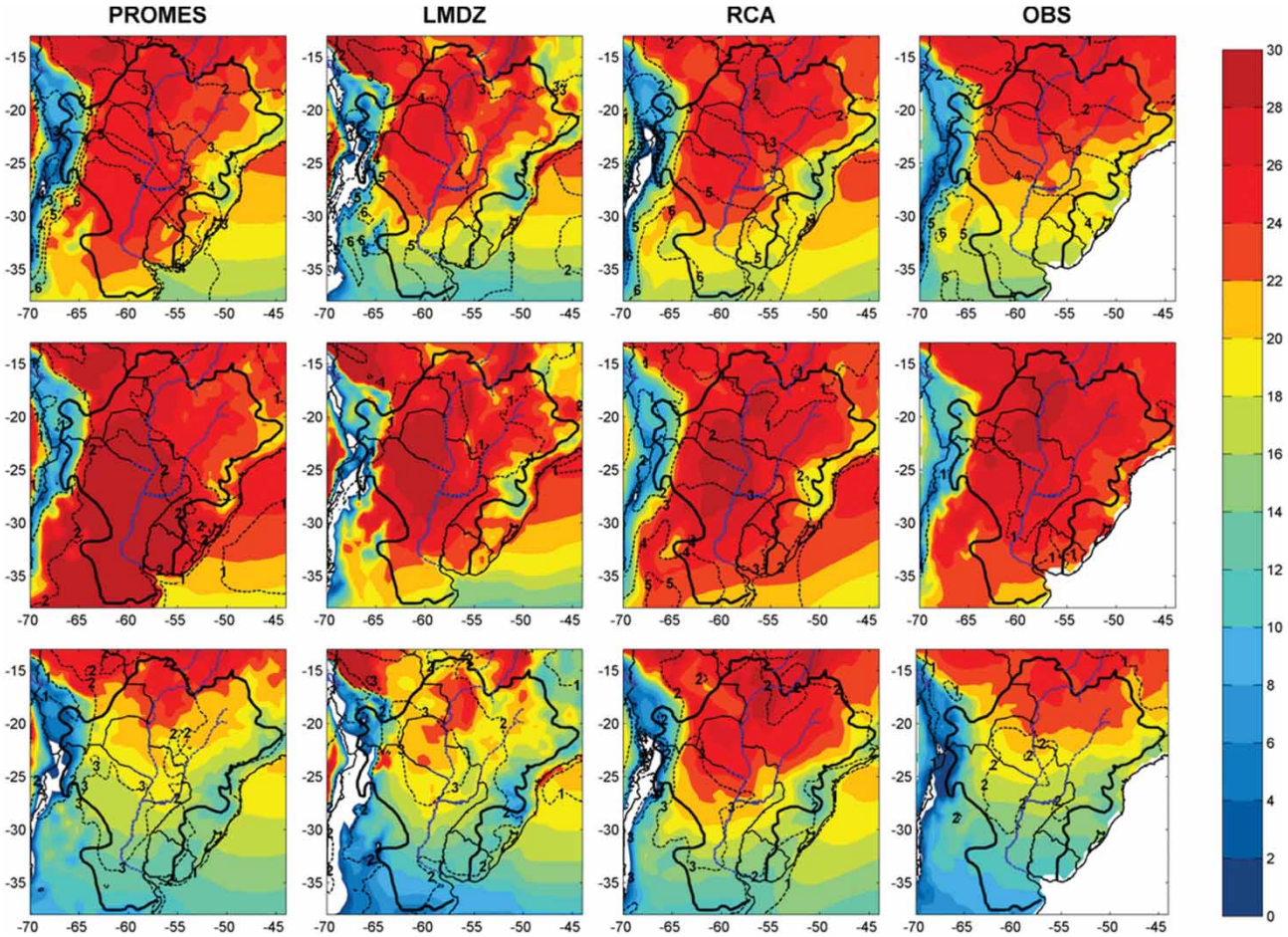

Figure 2 As in Figure 1 but for mean temperature. Units are °C. Values lower than 0°C are depicted in white. In the observations, areas over the Atlantic Ocean have been blanked out and are also displayed in white.

cycle by means of a grid-point representation of soil type and land cover along with a sub-grid parameterization for processes related to infiltration. The model's inputs are information on soil type, topography and vegetation, as well as daily information on selected meteorological variables. Its skill to simulate the main hydrologic features of various basins worldwide has been proved extensively (Mattheussen *et al*. 2000, Wood *et al*. 2002) and it has already been applied to LPB as well (Su and Lettenmaier 2009, Saurral 2010).

In this study, soil data were derived from the five-minute Global Soil Data Task data set taken from the Distributed Active Archive Center (2000), and vegetation information was obtained from the University of Maryland's 1-km Global Land Cover product (Hansen *et al*. 2000). The meteorological information used to force the model were daily minimum and maximum temperature, precipitation, wind speed, relative humidity and long- and short-wave incoming radiation in periods 1991–2000, 2021–2040 and 2071–2090 obtained from each RCM. The inclusion of information on relative humidity and radiation is relevant, given that Pierce *et al*. (2013) showed that spurious humidity trends can be obtained in VIC when humidity is parameterized with temperature, precipitation and wind speed alone (Kimball *et al*. 1997, Thornton and Running 1999, Bohn *et al*. 2013), resulting in trends opposite to those of the RCMs.

Spatial resolution for VIC was selected at 1/8 degree, and soil, land cover and meteorological information was re-gridded to that resolution. All simulations were performed with a time step of 24 h and in water balance mode which does not solve the surface energy balance, but considers instead that soil temperature is equal to the air temperature for any given time step. As this basin lies in a subtropical climate and does not register frozen precipitation or freezing of the water bodies, all modules related to snow and melting/sublimation processes in the model were not included.

Calibration of the hydrologic model consists of tuning selected parameters related to physical properties of the basin. Broadly speaking, calibration is done mainly on five specific parameters of the model: *Dsmax* (the maximum baseflow that can occur from the lowest soil layer in mm day^{-1}), *Ds* (the fraction of *Dsmax* where nonlinear baseflow begins), *Ws* (the fraction of the maximum soil moisture of the lowest soil layer where nonlinear baseflow occurs), b_{inf} (which defines the shape of the VIC curve) and the soil depth of each of the layers. In particular, calibration in this paper was performed by adjusting the infiltration capacity parameter b_{inf} and the depths of each of the three

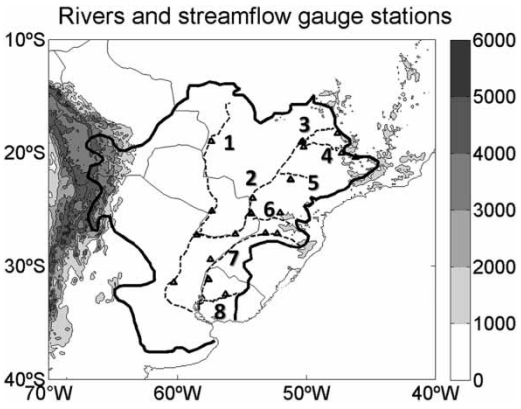

Figure 3 Location of the rivers and closing points considered in this paper. 1 = Paraguay River; 2 = Paraná River; 3 = Paranaíba River; 4 = Grande River; 5 = Paranapanema River; 6 = Iguazú River; 7 = Uruguay River; and 8 = Negro River. The topography of the basin in metres is shown in shading.

layers in which soil is divided in VIC. b_{inf} defines the shape of the infiltration curve in the model and describes the amount of available infiltration capacity as a function of gridcell area under saturation, while thicker soil depths lead to slower runoff and increases the water loss due to evapotranspiration. More details on the calibration of the VIC model over LPB have been documented in previous papers (Su and Lettenmaier 2009, Saurral 2010). It is important to mention that although VIC outputs consist of surface and sub-surface runoff which can be converted into discharges using a routing scheme (Lohmann *et al*. 1996, 1998) at daily, monthly and annual time scales, analysis in this paper concentrates only on the monthly data, given that the objective is to derive seasonal and annual variations in streamflow due to climate change.

Figure 3 displays the location of the rivers and the observed temperature/precipitation gauge stations considered and Table 2 lists the closing points for which future streamflow scenarios are derived. Most of the closing points are located in the Paraná, Uruguay and Paraguay rivers, the three largest in the basin, while other gauge stations lie in some of their tributaries. Previous works (Su and Lettenmaier 2009, Saurral 2010) found that VIC performs best in LPB in the Paraná and Uruguay rivers, which are characterized by rapid responses of runoff to precipitation, while its skill to simulate the Paraguay and other slow rivers is noticeably lower.

2.3 *RCMs correction scheme*

Several authors have proposed statistical methods to remove the errors found in climate simulations, mainly to increase their utility in impact studies (Vidal and Wade 2007, 2008, 2009, Teutschbein and Seibert 2012, Piani and Haerter 2012). In this paper, systematic errors in precipitation and temperature fields are corrected by means of the application of a statistical unbiasing scheme known as 'quantile-based mapping' which uses the statistical distributions of both variables and follows the method proposed by Wood *et al*. (2002). The scheme first requires the computation of the percentile distributions of precipitation and mean temperature in the observations and each RCMs' present climate. Once the percentile distributions of both variables are derived, each future month in each RCM is

Table 2 Closing points location and observed annual mean streamflow (Q_{mean}, in $m^3\ s^{-1}$)

Station number	Station name	River	Latitude (°)	Longitude (°)	Q_{mean} ($m^3\ s^{-1}$)
1	Corrientes	Paraná	−27.27	−58.49	17,101
2	Paso de los Libres	Uruguay	−29.43	−57.42	4428
3	Paraná	Paraná	−31.46	−60.28	14,119
4	Asunción	Paraguay	−25.15	−57.31	3222
5	Posadas	Paraná	−27.20	−55.50	12,539
6	Ladario	Paraguay	−19.00	−57.35	1291
7	Fazenda Santa Fe	Paranaíba	−19.08	−50.37	75
8	Rifaína	Grande	−20.05	−47.23	1059
9	Salto Grande	Uruguay	−22.39	−51.20	4716
10	Guaira	Paraná	−24.04	−54.14	9470
11	Salto Caxias	Iguaçu	−25.40	−54.25	1912
12	Iraí	Uruguay	−27.11	−53.15	1515
13	Salto Osorio	Iguaçu	−25.31	−52.01	1034
14	Itaipú	Paraná	−25.30	−54.30	10,130
15	Furnas	Grande	−20.39	−46.18	924
16	Agua Vermelha	Grande	−19.51	−50.20	2089
17	Emborcacao	Paranaíba	−18.27	−47.59	486
18	Itá	Uruguay	−27.16	−52.23	1043
19	Rincón del Bonete	Negro	−32.50	−56.25	579
20	Balsa do Paranapanema	Paranapanema	−31.17	−57.56	978

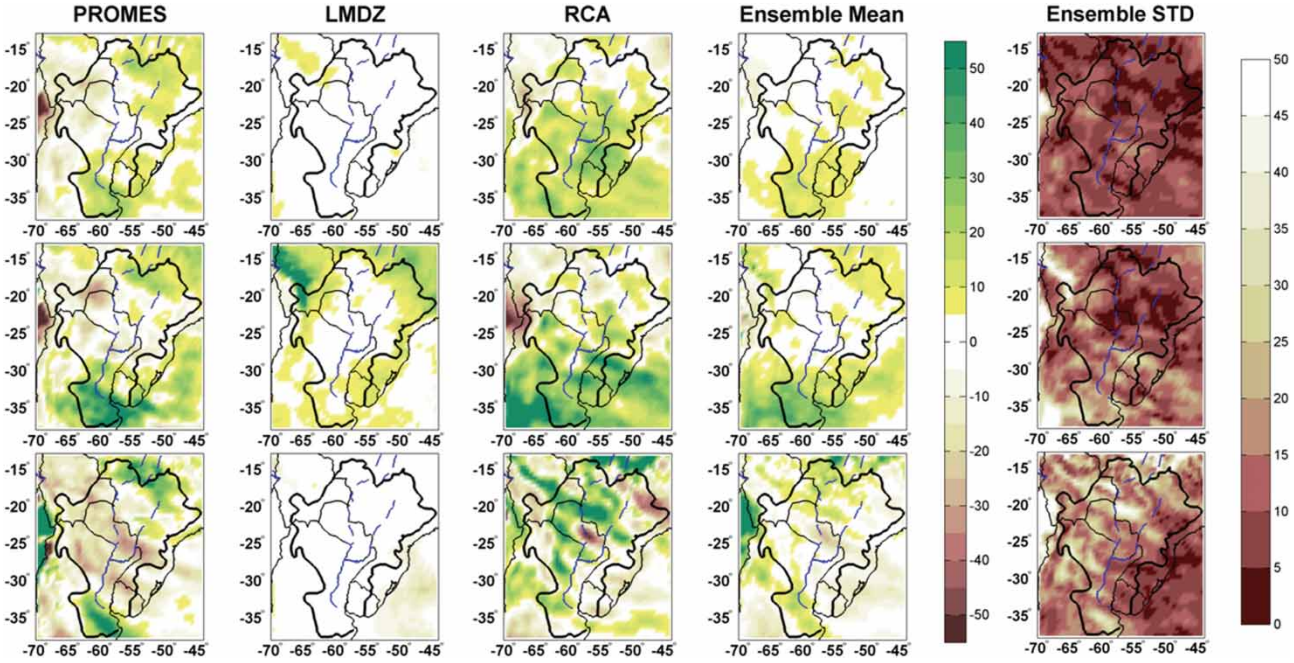

Figure 4 Percent difference in annual (top), DJF (middle) and JJA (bottom) mean precipitation for period 2021–2040 with respect to the present climate in PROMES, LMDZ and RCA (first to third column, respectively). The fourth and fifth columns show the ensemble mean and standard deviation computed using the three RCMs.

assigned its corresponding *i*-th percentile in the RCM distribution and the same *i*-th percentile but now in the observations is found. In the case of temperature, the monthly mean future value is corrected by adding to the value the difference between the *i*-th percentile in the observations and the *i*-th percentile in the RCM. In the case of precipitation, each monthly value is corrected by multiplying the value of the monthly precipitation by the ratio between the *i*-th percentile of rainfall in the observations and the *i*-th percentile in the RCM. In a statistical sense, this method aims to keep the RCM

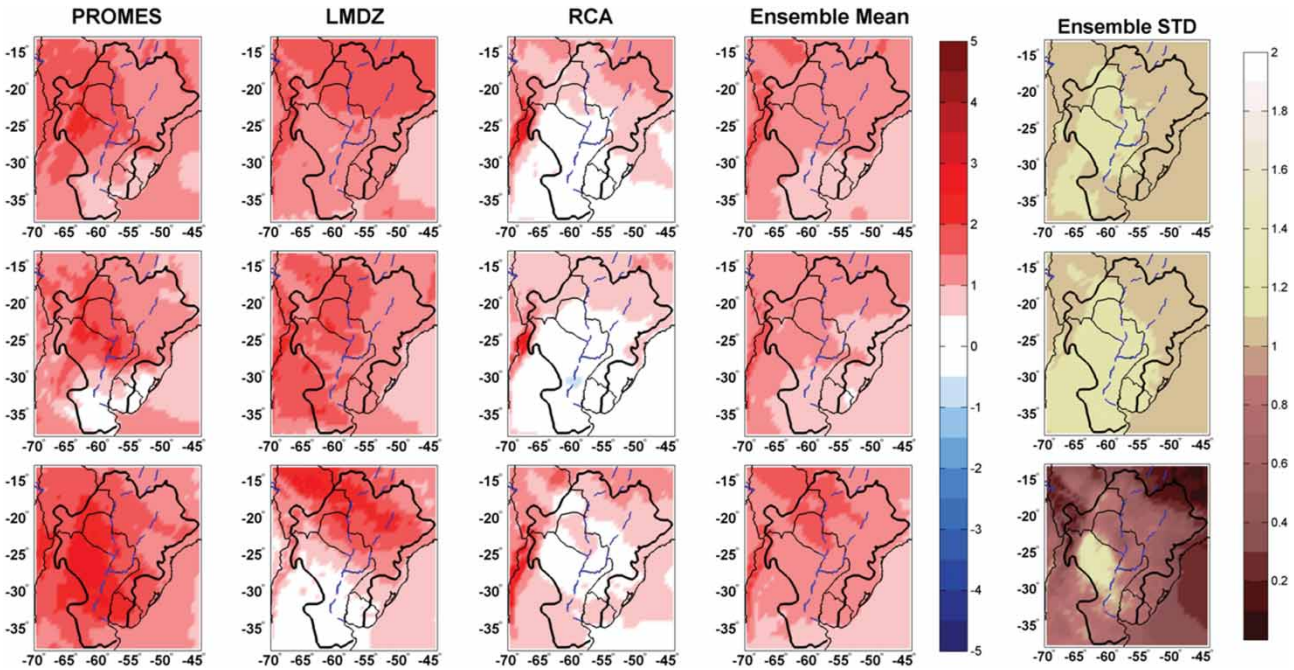

Figure 5 Difference in annual (top), DJF (middle) and JJA (bottom) mean temperature for period 2021–2040 with respect to the present climate in PROMES, LMDZ and RCA (first to third column, respectively). The fourth and fifth columns show the ensemble mean and standard deviation. Units are °C.

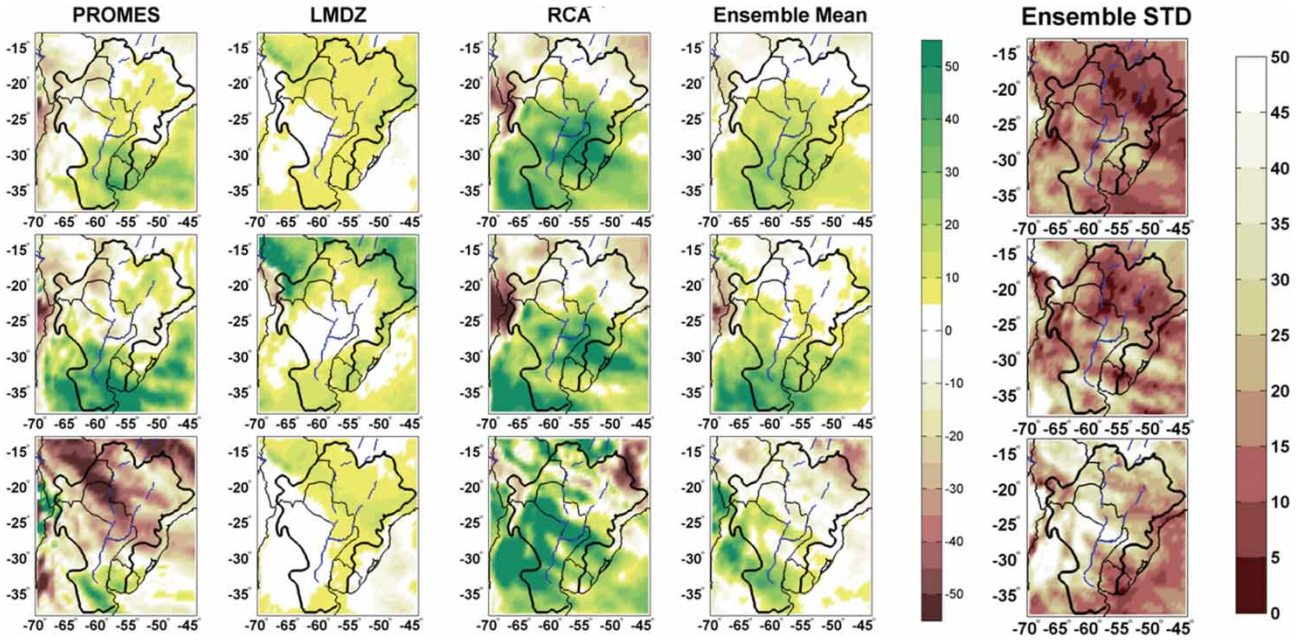

Figure 6 As in Figure 4 but for period 2071–2090.

precipitation and temperature distributions close to the observed ones, and it not only makes a correction in the mean values – as several unbiasing schemes do – but also takes into account the variance, kurtosis, asymmetry and other higher-order distribution momenta as well. This method was already found to be adequate to remove systematic climate biases in impact studies on LPB using GCMs (see Saurral 2010), but this is the first time that it has been used to improve RCM simulations for hydrologic impact assessment in this region.

Results of the application of the unbiasing scheme on RCM data over selected sub-basins are quantified by the computation of the normalized root mean square error (NRMSE), defined as follows:

$$\mathrm{NRMSE} = \frac{\sqrt{\sum_{i=1}^{n} \left(x_i^{\mathrm{OBS}} - x_i^{\mathrm{SIM}}\right)^2 / n}}{\sqrt{\sum_{i=1}^{n} \left(x_i^{\mathrm{OBS}}\right)^2 / n}},$$

where x_i^{OBS} and x_i^{SIM} denote the observed and simulated variable x at time i and n accounts for the sample size.

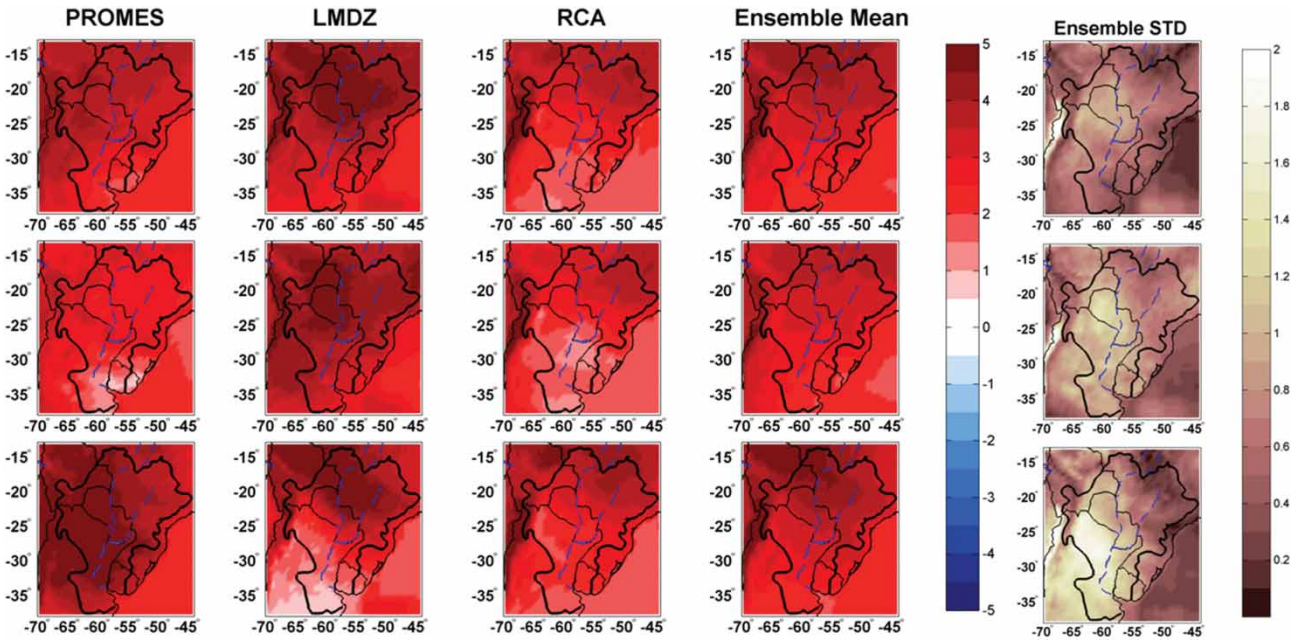

Figure 7 As in Figure 5 but for period 2071–2090.

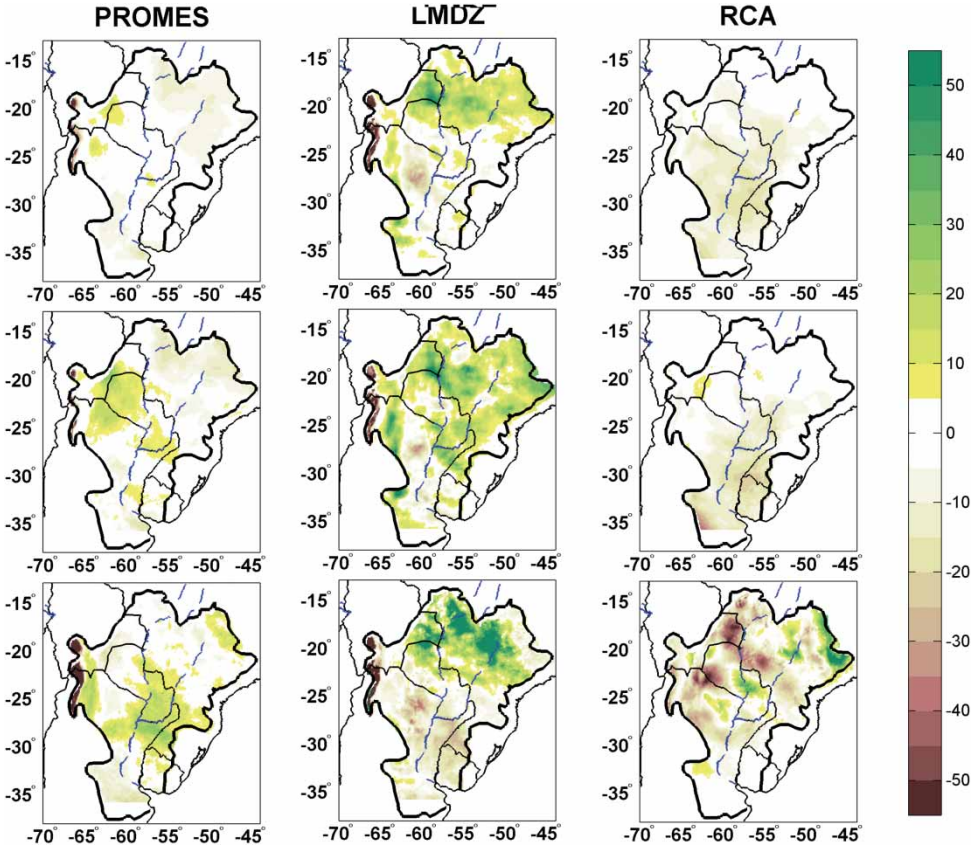

Figure 8 Percent difference in annual (top), DJF (middle) and JJA (bottom) mean evapotranspiration for the period 2021–2040 with respect to the present climate in PROMES, LMDZ and RCA (first to third column, respectively).

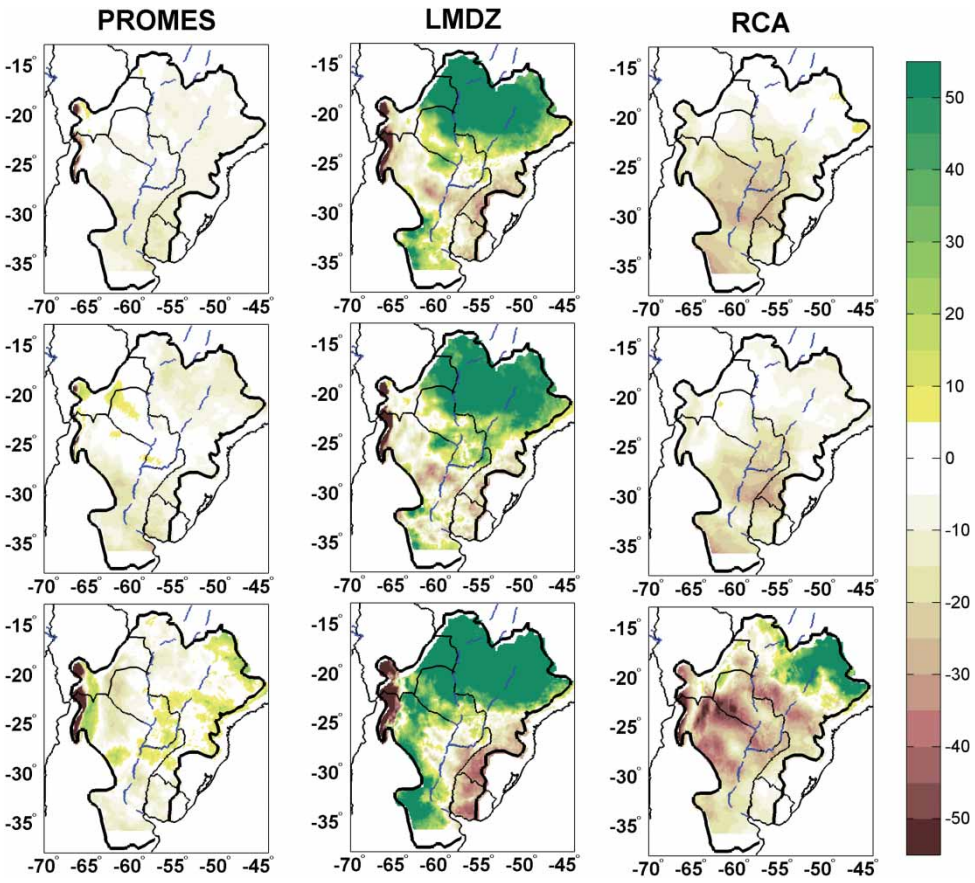

Figure 9 As in Figure 8 but for period 2071–2090.

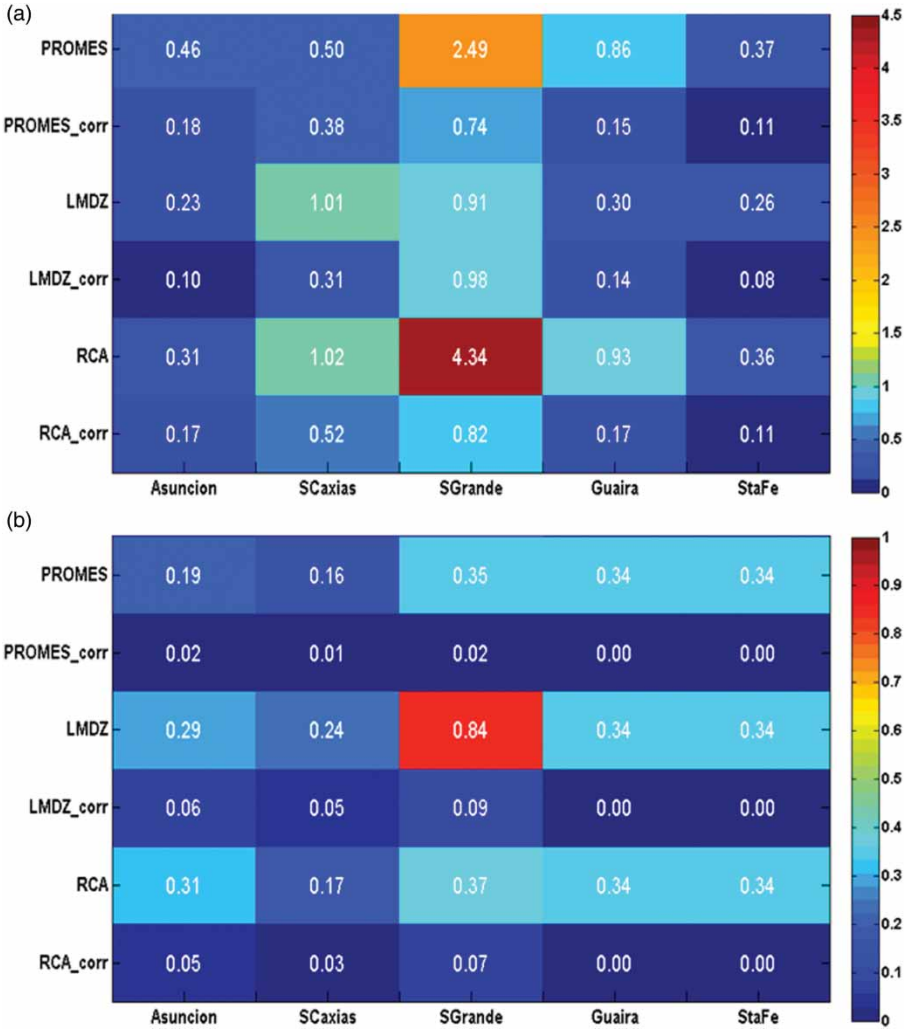

Figure 10 NRMSE of annual time series of (a) precipitation, and (b) temperature in (from top to bottom) PROMES, PROMES corrected with quantile mapping, LMDZ, LMDZ corrected, RCA and RCA corrected, validated against observations taken from CRU. Results are shown for five random closing points, namely Asunción, Salto Caxias, Salto Grande, Guaira and Santa Fe (from left to right).

3 Results and discussion

3.1 *Future climate*

Figure 4 depicts the variations in annual, summer and winter mean precipitation for 2021–2040 with respect to the current climate in PROMES, LMDZ and RCA along with the ensemble mean and standard deviation to facilitate the detection of 'hot spots' of change (i.e. regions where the RCMs simulate a similar variation). The annual field is quite different among the RCMs although there is a trend towards more rain in the southern half of the basin, which is particularly noticeable in the RCA and PROMES models. LMDZ, on the other hand, shows very little variation, less than 10% either up or down, across all LPB. Over the northern part, there are discrepancies on the future scenarios, with RCA and PROMES predicting more rain and LMDZ simulating less rain for the near future. Differences also exist over the west of LPB, with RCA predicting increases in annual rainfall of nearly 10–20%, almost no change in LMDZ and a drying trend in PROMES. In the seasonal means, a clear pattern of increased precipitation on the southern half of the basin is found in summer (which is expected for all RCMs), while in winter, the signal is much less clear on LPB and depends markedly on the RCM. It is interesting to note that the signal of slightly more rainfall over southern Brazil is about 20–25°S in the annual and summer fields is coherent among the models as there is also a minimum in standard deviation. On the other hand, the expected increase in rainfall over the southern half of the basin is less confident, as standard deviation values there are larger, particularly in the cold season. Whether this increase in rainfall is related or not to an increase in baroclinic activity – the main contributor to rainfall in that region – is beyond the scope of this paper but will be analysed in future works.

Variations in temperature for the near future (Figure 5) are characterized by a clear warming trend in all models. However, the magnitude of the warming markedly differs across RCMs varying from almost 3°C in the annual mean in the central part

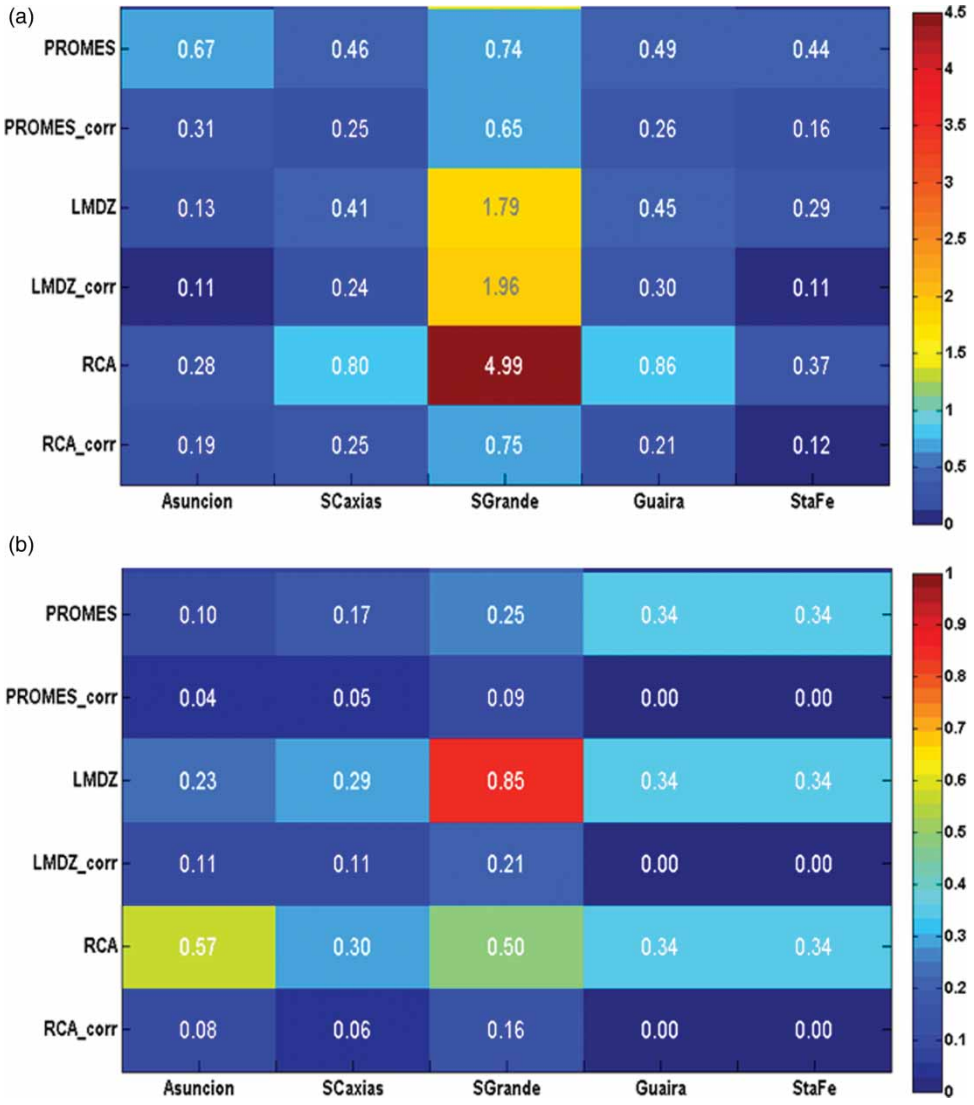

Figure 11 As in Figure 10 but for summer.

of the basin in PROMES to less than 1°C in the same region in RCA. Differences across RCMs also exist in the seasonal analysis. For example, RCA predicts a cooling of between 0.5°C and 1°C over central-southern LPB during the summer, though this is the only model that predicts a negative temperature change over the region. As in the case of precipitation, the expected variations in temperature appear more confident over the central and northern parts of the basin, as standard deviation values once again maximize over central and northern Argentina.

For the far future (2071–2090; Figure 6), the increase in rainfall is larger during all seasons in the southern parts, being most clear in summer. During winter, the central and northern parts of the basin are predicted to have less rainfall in PROMES and slightly more precipitation in the other two RCMs. LMDZ is the model depicting the smallest variations in mean precipitation. Standard deviation analysis indicates variations in precipitation for 2071–2090 are most likely to occur over the northern part of the basin, while changes in the southern half appear less homogeneous among ensemble members.

In terms of temperature (Figure 7), the whole basin would experience warmer temperatures than in the current climate as shown by all RCMs, although these changes are most likely north of about 20°S. Changes in the southern and southwestern parts of the basin are much less variable between members, resulting in larger standard deviation values. Despite the differences in magnitude depending on the RCM and the region analysed, these models mostly agree in projecting a moderate warming of LPB by the end of this century.

Figures 8 and 9 show variations in annual, summer and winter mean evapotranspiration in periods 2021–2040 and 2071–2090, respectively, with respect to the present climate. For 2021–2040, PROMES predicts changes generally bounded between −30% and 30%, with positive changes (increased evapotranspiration) over the central and western parts of the basin in summer and winter. At the same time, LMDZ indicates more evapotranspiration in the northern half of the basin in the annual field and also in the two seasons, while RCA shows small reductions in the evapotranspiration

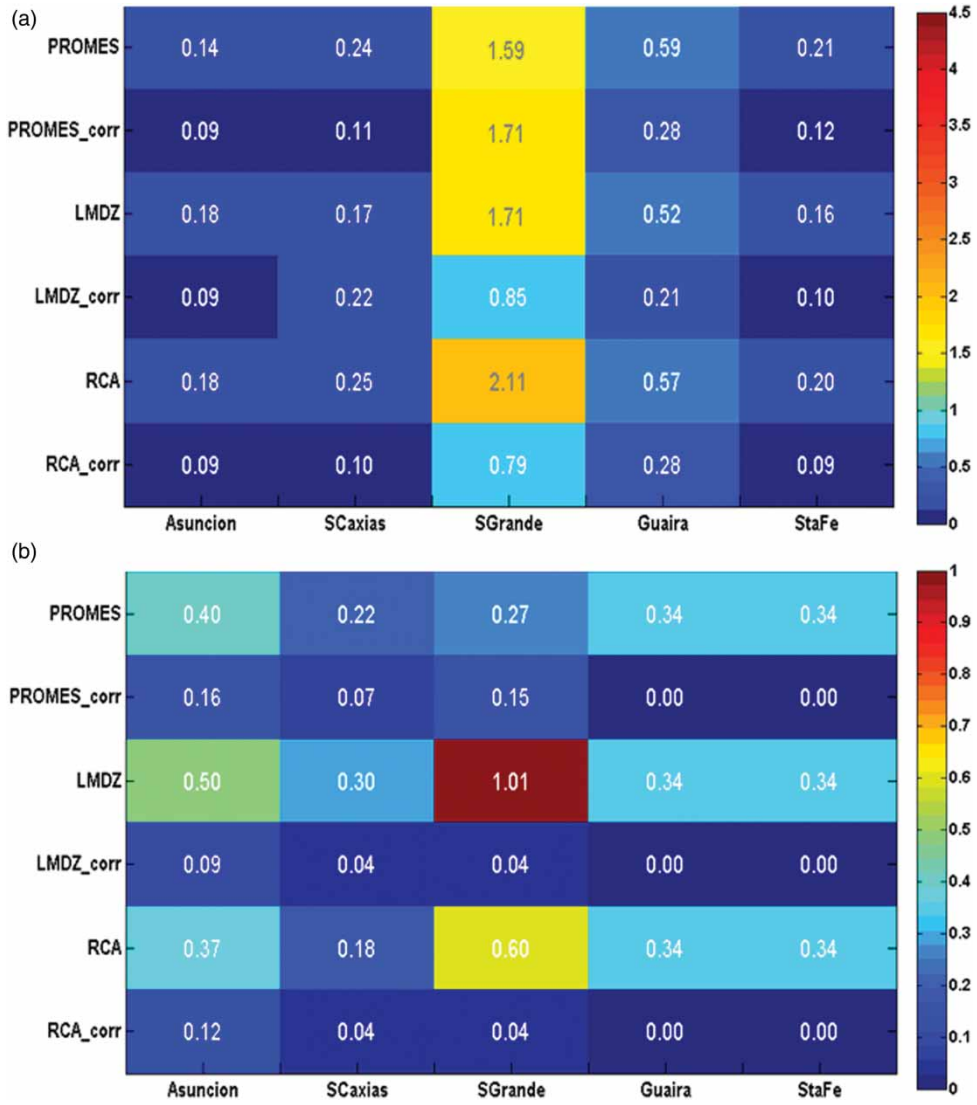

Figure 12 As in Figure 10 but for winter.

over much of the basin, but with values no larger than 20% except for winter where changes of up to −40% are found. When the period 2071–2090 is considered, variations in PROMES are very small but LMDZ increases evapotranspiration markedly between 15°S and 25°S and reduces evapotranspiration over the southeastern part of the basin. RCA keeps its drying trend over much of the basin with larger values compared to period 2021–2040. However, this RCM predicts an increase in evapotranspiration over the northeastern edge of the basin during the cold season.

3.2 *Unbiasing of RCM data*

The application of the quantile-based mapping technique to the RCM data leads to a noticeable improvement in the simulations. This is particularly important in this study, given that errors in temperature or precipitation fields are immediately transferred into the hydrologic field, reducing the confidence of the future hydrology scenarios. Figures 10–12 display NRMSE values for annual, summer and winter time series, respectively, of precipitation (top) and temperature (bottom) before and after the application of the unbiasing scheme and for five selected sub-basins with closing points at the Asunción, Salto Caxias, Salto Grande, Guaira and Santa Fe regions. All the grid points falling inside each sub-basin were averaged and used to derive the observed and simulated time series. In the case of annual means (Figure 10), nearly all the simulations reduce their NRSME values after the unbiasing method except for LMDZ for precipitation in the Salto Grande sub-basin. The method does a remarkable job in many of the basins, as in the case of the Salto Grande region for RCA where NRSME is reduced from 4.34 to less than 1. In summer (Figure 11), there are also noticeable improvements over the vast majority of the regions and RCMs except for the LMDZ model in the Salto Grande sub-basin. In winter (Figure 12), all simulations are improved with the application of the unbiasing scheme except for the PROMES precipitation in Salto Grande, with the largest improvement seen in LMDZ and RCA for temperature.

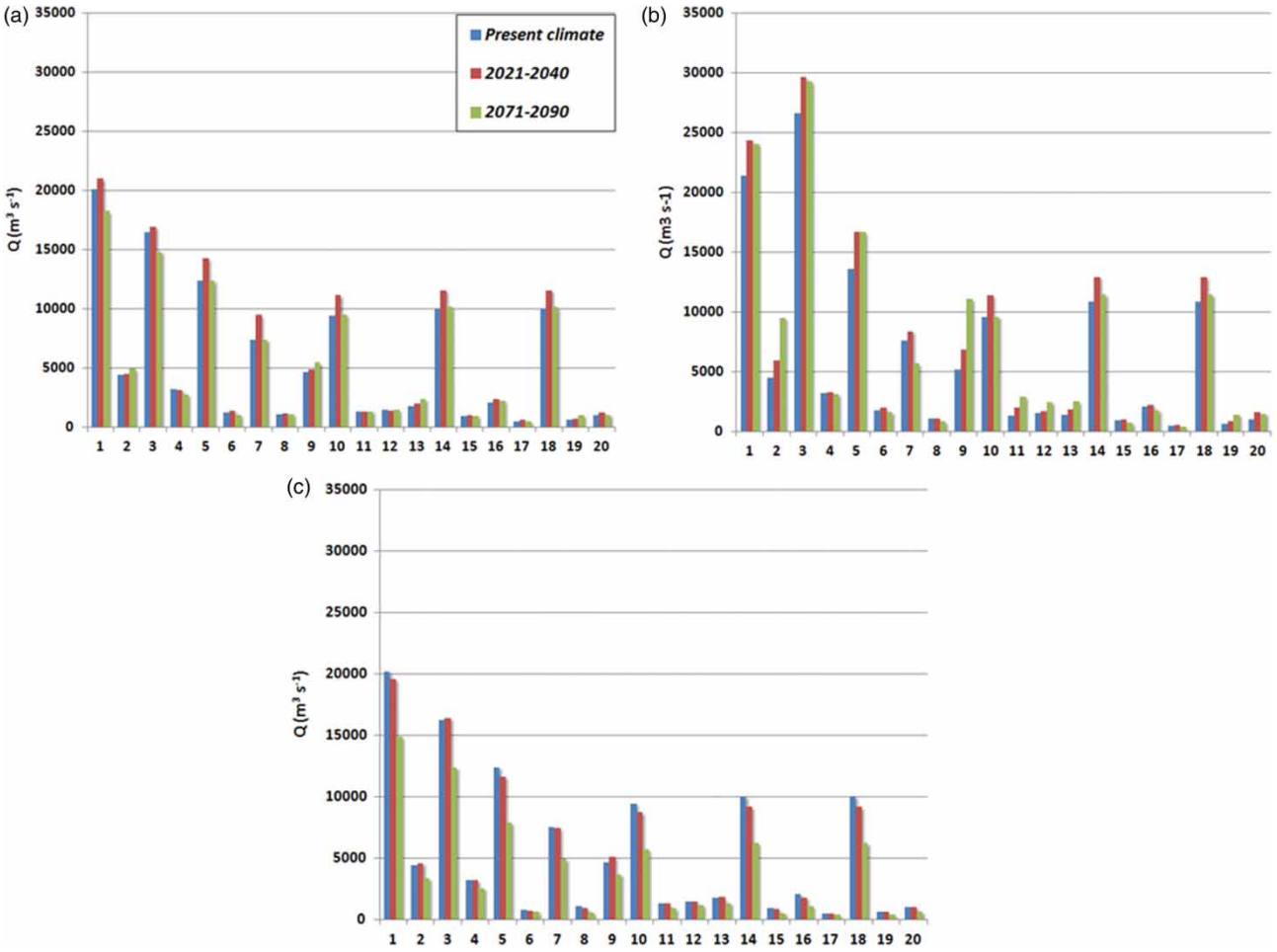

Figure 13 Mean streamflow at the 20 gauge stations (see list in Table 2) in the present climate (blue bars), the 2021–2040 period (red bars) and the 2071–2090 period (light green bars) in units of $m^3\ s^{-1}$ in (a) PROMES; (b) RCA; and (c) LMDZ. Note that streamflow at station 7 (Fazenda Santa Fe) has been scaled by a factor of 100 to be discernible in the scale used in the figure.

3.3 *Future hydrology scenarios*

Even when temperature, precipitation and evapotranspiration projections for the upcoming decades show differences across RCMs, VIC simulations forced with bias-free meteorological data could provide a fruitful tool for impact studies on water management and availability in LPB. Figure 13 shows VIC outputs of mean streamflow at the 20 selected closing points listed in Table 2 for the present climate, near future and far future, according to each RCM. In the case of the Paraná River, all three RCMs depict a similar pattern characterized by an increase in streamflow in the near future followed by a declining trend towards the end of the century for most of the closing points. In general, fluctuations either up or down in streamflow for the Paraná River, which accounts for the largest streamflow in the basin, are predicted to be less than 10% from the present time into the future according to the RCM scenarios. The largest differences are found for the end of the century with streamflow predictions at Corrientes in the Paraná River ranging from 18,000 $m^3\ s^{-1}$ (LMDZ) to 24,000 $m^3\ s^{-1}$ (RCA). These scenarios have a larger-than-average confidence, given that the sub-basin lies in the region with low ensemble standard deviations. For the Uruguay River, RCMs mostly predict increased streamflow for the next decades except for the LMDZ model which simulates slightly larger discharges in the near future followed by a reversal towards lower values, getting back to conditions similar to those of the present climate. RCA predicts increased streamflow at the Middle and Lower Uruguay River (i.e. Salto Grande, Paso de los Libres) for the two future periods and an increase followed by a decrease for the Upper Paraná (i.e. Itá).

Figure 14 shows the magnitude of the largest positive streamflow extremes, for the three time slices and the four RCMs. In general, the pattern is quite similar to that of differences in the mean values depicted in Figure 13, but in some cases (e.g. Posadas, in the Paraná River), extreme values attain a maximum when compared to the other locations in PROMES. Interestingly, the magnitude of the largest streamflow in PROMES should be expected by the end of the period (2071–2090) for most of the sub-basins, while at the same time RCA and LMDZ predict largest streamflow by 2021–2040 followed by a decrease towards the end of the present century. As expected, the potential errors in predicting extremes (both magnitude and timing) are even larger than in the mean values, so

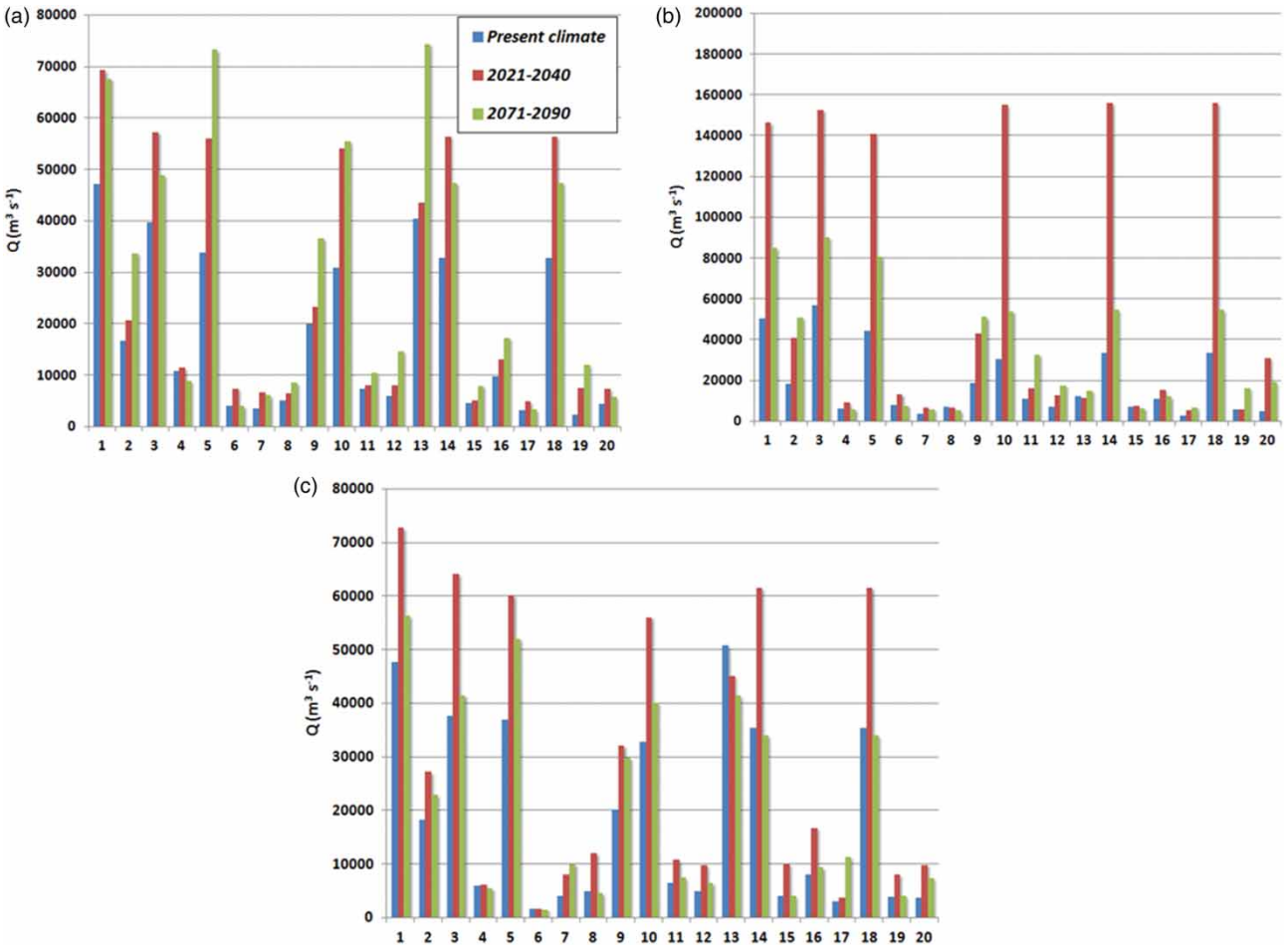

Figure 14 As in Figure 13 but for the largest monthly streamflow in the series. Note that panels have different vertical scales and that streamflow at station 7 (Fazenda Santa Fe) has been scaled by a factor of 10 to be discernible in the scales used in the figure.

these results should be taken with care and considered only in the framework of a possible future hydrologic scenario over South America.

4 Conclusions

In this study, simulation outputs taken from a set of three RCMs have been used to force the VIC hydrologic model. As RCMs have biases in their mean atmospheric fields and this precludes their direct use for impact assessments, a statistical scheme to remove the systematic part of the bias was used. The statistical bias correction of the systematic errors considered allowed producing long-term flows time series with a statistical distribution close to that of the observations to make them applicable as input for the hydrology model. This methodology was used in hydrologic assessment in previous studies, including the LPB region (Saurral 2010, Camilloni *et al*. 2013, Montroull *et al*. 2013). The VIC model was then forced with the bias-corrected data and results were found to be close to the observations in the present climate.

Future hydrologic scenarios were also derived, considering RCM data for the periods 2021–2040 (near future) and 2071–2090 (far future). In terms of climate projections, RCMs predict warmer conditions in almost the whole basin (with the exception of the RCA model on central LPB for the period 2021–2040), being particularly large for the end of the century, while precipitation variations are less uniform across RCMs. The variation in evapotranspiration is not uniform when the three RCMs are analysed, but overall a weak trend towards increased evapotranspiration could be identified over the northern part of the basin for the next decades. This scenario is particularly favoured by LMDZ. The majority of the RCMs coincide to project more rainfall in the southern half of the basin, but over the central and northern parts (where much of runoff originates) the variation patterns are less uniform. As can be expected, the fact that the RCMs used in this paper are (as in most cases) largely driven by variations in the climate of the GCMs that provide the BC, the large-scale variations in precipitation and temperature are pretty much the same to those predicted by these GCMs. Then, differences in the projection of rainfall changes among RCMs are comparable to those among GCMs (Saurral 2010, Montroull *et al*. 2013).

In general, a trend towards a gradual increase in streamflow was found for the majority of the rivers in the basin. PROMES and LMDZ are associated with increased flows in the near

future followed by a negative trend, leading in consequence to only minor changes by the end of the century with respect to the current conditions. Future changes in the largest monthly streamflow are similar to those in the mean values, with also some differences among RCMs and in the sub-basins considered.

There is an increasing demand for future climate scenarios, particularly for impact studies. Despite the uncertainties in regional climate projections, these findings could be relevant to be used in impact assessments of climate change in LPB that could provide planners and water resources managers with information to make decisions about meeting demands, flood risks and ecosystems fragility in the future.

Funding

This research was supported by the European Community's Seventh Framework Programme (FP7/2007–2013) under grant agreement number 212492, the University of Buenos Aires UBACYT-20020100100803, Consejo Nacional de Investigaciones Científicas y Técnicas PIP2009-00444 and Agencia Nacional de Promoción Científica y Tecnológica PICT07-00400.

References

Barros, V., *et al*., 2004. The major discharge events in the Paraguay River: magnitudes, source regions and climate forcings. *Journal of Hydrometeorology*, 5, 1161–1170.

Barros, V., Doyle, M., and Camilloni, I., 2008. Precipitation trends in southeastern South America: relationship with ENSO phases and with low-level circulation. *Theoretical and Applied Climatology*, 93, 19–33.

Bischoff, S., *et al*., 2000. Climatic variability and Uruguay River flows. *Water International*, 25, 446–456.

Bohn, T.J., *et al*., 2013. Global evaluation of MTCLIM and related algorithms for forcing of ecological and hydrological models. *Agricultural and Forest Meteorology*, 176, 38–49. doi:10.1016/j.agrformet.2013.03.003.

Camilloni, I., Saurral, R., and Montroull, N., 2013. Hydrological projections of fluvial floods in the Uruguay and Paraná basins under different climate change scenarios. *International Journal of River Basin Management*, 11 (4), 389–399.

Castañeda, M.E. and Barros, V., 1994. Las tendencias de la precipitación en el Cono Sur de América al este de los Andes. *Meteorológica*, 19, 23–32.

Distributed Active Archive Center, 2000 *Global soil data products (IGBP-DIS)* [online]. Oak Ridge National Laboratory Distributed Active Archive Center [CD-ROM]. Available from: http://daac.ornl.gov/SOILS/igbp.html [Accessed November 2005].

Domínguez, M., *et al*., 2010. A regional climate model simulation over West Africa: parameterization tests and analysis of land-surface fields. *Climate Dynamics*, 35, 249–265.

Doyle, M. and Barros, V.R., 2011. Attribution of the river flow growth in the Plata Basin. *International Journal of Climatology*, 31, 2234–2248.

Doyle, M., Saurral, R., and Barros, V., 2012. Trends in the distributions of aggregated monthly precipitation over the La Plata Basin. *International Journal of Climatology*, 32, 2149–2162.

Grimm, A., Barros, V., and Doyle, M., 2000. Climate variability in southern South America associated with El Niño and La Niña events. *Journal of Climate*, 13, 35–58.

Gulizia, C., Camilloni, I., and Doyle, M., 2012. Identification of the principal patterns of summer moisture transport in South America and their representation by WCRP/CMIP3 global climate models. *Theoretical and Applied Climatology*, 112, 227–241. doi:10.1007/s00704-012-0729-4.

Hansen, M.C., *et al*., 2000. Global land cover classification at 1 km resolution using a classification tree approach. *International Journal of Remote Sensing*, 21, 1331–1364.

Hourdin, F., *et al*., 2006. The LMDZ4 general circulation model: climate performance and sensitivity to parametrized physics with emphasis on tropical convection. *Climate Dynamics*, 27, 787–813.

Kimball, J.S., Running, S.W., and Nemani, R.R., 1997. An improved method for estimating surface humidity from daily minimum temperature. *Agricultural and Forest Meteorology*, 85 (1–2), 87–98. doi:10.1016/S0168-1923(96)02366-0.

Kjellström, E., *et al*., 2005. A 140-year simulation of European climate with the new version of the Rossby Centre regional atmospheric climate model (RCA3). Report in Meteorology and Climatology 108, SMHI, SE-60176 Norrköping, Sweden, 54 pp.

Kodama, Y.M., 1992. Large-scale common features of sub-tropical precipitation zones (the Baiu Frontal Zone, the SPCZ, and the SACZ). Part I: characteristics of subtropical frontal zones. *Journal of the Meteorological Society of Japan*, 70, 813–835.

Li, Z.X., 1999. Ensemble atmospheric GCM simulation of climate interannual variability from 1979 to 1994. *Journal of Climate*, 12, 986–1001.

Liang, X., *et al*., 1994. A simple hydrologically based model of land surface water and energy fluxes for GSMs. *Journal of Geophysical Research*, 99 (7), 14415–14428.

Liang, X., Lettenmaier, D.P., and Wood, E.F., 1996. One-dimensional statistical dynamic representation of subgrid spatial variability of precipitation in the two-layer variable infiltration capacity model. *Journal of Geophysical Research*, 101 (16), 21403–21422.

Lohmann, D., Nolte-Holube, R., and Raschke, E., 1996. A large-scale horizontal routing model to be coupled to land surface parameterization schemes. *Tellus*, 48A, 708–721.

Lohmann, D., *et al*., 1998. Regional scale hydrology: 1. Formulation of the VIC-2 L model coupled to a routing scheme. *Hydrological Sciences Journal*, 43, 131–141.

Mattheussen, B., *et al*., 2000. Effects of land cover change on streamflow in the interior Columbia River Basin (USA and Canada). *Hydrological Processes*, 14, 867–885.

Mitchell, T.D. and Jones, P., 2005. An improved method of constructing a database of monthly climate observations and associated high-resolution grids. *International Journal of Climatology*, 25, 693–712.

Montroull, N., *et al*., 2013. Assessment of climate change on the future water levels of the Iberá wetlands, Argentina, during the 21st century. *International Journal of River Basin Management*, 11 (4), 401–410.

Nijssen, B.N., *et al.*, 1997. Streamflow simulation for continental-scale river basins. *Water Resources Research*, 33, 711–724.

Piani, C. and Haerter, J.O., 2012. Two dimensional bias correction of temperature and precipitation copulas in climate models. *Geophysical Research Letters*, 39, 1–5.

Pierce, D.W., Westerling, A.L., and Oyler, J., 2013. Future humidity trends over the western United States in the CMIP5 global climate models and the variable infiltration capacity hydrological modeling system. *Hydrology and Earth System Sciences*, 17, 1833–1850. doi:10.5194/hess-17-1833-2013.

Popescu, I., *et al*., 2012. Assessing residual hydropower potential of the La Plata Basin accounting for future user demands. *Hydrology and Earth System Sciences*, 16, 2813–2823.

Ropelewski, C.H. and Halpert, S., 1987. Global and regional scale precipitation patterns associated with the El Niño/Southern Oscillation. *Monthly Weather Review*, 115, 1606–1626.

Samuelsson, P., Gollvik, S., and Ullerstig, A., 2006. The land-surface scheme of the Rossby Centre regional atmospheric climate model (RCA3). Report in Meteorology 122. SMHI, SE-60176 Norrköping, Sweden, 25 pp.

Sanchez, E., *et al*., 2007. Impacts of a change in vegetation description on simulated European summer present-day and future climates. *Climate Dynamics*, 29, 319–332.

Saurral, R.I., 2010. The hydrologic cycle of the La Plata Basin in the WCRP/CMIP3 multi-model dataset. *Journal of Hydrometeorology*, 11, 1083–1102.

Silvestri, G.E. and Vera, C.S., 2003. Antarctic oscillation signal on precipitation anomalies over southeastern South America. *Geophysical Research Letters*, 30, 1–4.

Solomon, S., *et al*., eds., 2007. *Climate change 2007: the physical science basis*. United Kingdom and New York: Cambridge University Press, 996.

Su, F. and Lettenmaier, D.P., 2009. Estimation of surface water budget of La Plata Basin. *Journal of Hydrometeorology*, 10, 981–998.

Teutschbein, C. and Seibert, J., 2012. Bias correction of regional climate model simulations for hydrological climate-change impact studies: review and evaluation of different methods. *Journal of Hydrology*, 456–457, 12–29.

Thornton, P.E. and Running, S.W., 1999. An improved algorithm for estimating incident daily solar radiation from measurements of temperature, humidity, and precipitation. *Agricultural and Forest Meteorology*, 93 (4), 211–228. doi:10.1016/S0168-1923(98)00126-9.

Vera, C., Vigliarolo, P.K., and Berbery, E.H., 2002. Cold season synoptic-scale waves over subtropical South America. *Monthly Weather Review*, 130, 684–699.

Vera, C., *et al*., 2006. Climate change scenarios for seasonal precipitation in South America from IPCC-AR4 models. *Geophysical Research Letters*, 33, 1–4, L13707.

Vidal, J.-P. and Wade, S., 2007. A framework for developing high-resolution multi-model climate projections: 21st century scenarios for the UK. *International Journal of Climatology*, 28, 843–858.

Vidal, J.-P. and Wade, S., 2008. Multimodel projections of catchment-scale precipitation regime. *Journal of Hydrology*, 353, 143–158.

Vidal, J.-P. and Wade, S., 2009. A multimodel assessment of future climatological droughts in the United Kingdom. *International Journal of Climatology*, 29 (14), 2056–2071.

Wood, A.W., *et al*., 2002. Long-range experimental hydrologic forecasting for the eastern United States. *Journal of Geophysical Research*, 107, 4429–4443. doi:10.1029/2001JD000659.